Optical Materials 77 (2018) 233–239

Contents lists available at ScienceDirect

Optical Materials

journal homepage: www.elsevier.com/locate/optmat

Temperature-dependent emission color and temperature sensing behavior in $Tm^{3+}/Yb^{3+}:Y_2O_3$ nanoparticles

Guangrun Chen, Ruoshan Lei**, Huanping Wang, Feifei Huang, Shilong Zhao, Shiqing Xu*

College of Materials Science and Engineering, China Jiliang University, Hangzhou 310018, China

ARTICLE INFO

Article history:
Received 25 June 2017
Received in revised form
26 November 2017
Accepted 26 January 2018

Keywords:
Luminescence
Optical temperature sensor
Fluorescence intensity ratio
Nanoparticles

ABSTRACT

$Tm^{3+}/Yb^{3+}:Y_2O_3$ nanoparticles (NPs) were prepared by solution combustion method. The prepared NPs are confirmed to be pure cubic Y_2O_3 phase with the mean size of about 45 nm by X-ray diffraction (XRD) analysis and transmission electron microscopy (TEM) observation. Under 980 nm excitation, the temperature dependent upconversion (UC) emission spectra of the NPs are obtained. It is found that the NPs show color tunability with a variation in temperature (from blue to almost white) and also a relatively good suppression of temperature quenching (i.e. ~70.4% of the initial intensity at 473 K). By using the fluorescent intensity ratio (FIR) technique, the temperature sensing behaviors are investigated based on the thermal coupled $^1G_{4(a)}$ (477 nm) and $^1G_{4(b)}$ (490 nm) levels and non-thermal coupled $^3F_{2,3}$ (684 nm) and $^1G_{4(b)}$ (490 nm) levels from Tm^{3+} ions, respectively. The results demonstrate that both the absolute sensitivity (S_a) and relative sensitivity (S_r) values based on non-thermal coupled levels of $^3F_{2,3}$ and $^1G_{4(b)}$ is larger in the experimental temperature range. The maximum S_a and S_r values are obtained to be ~$1170 \times 10^{-4}\,K^{-1}$ at 573 K and ~$1.51\%K^{-1}$ at 445 K, respectively. Therefore, the studied material is a potential multifunctional composite for optical thermometry and temperature safety sign.

1. Introduction

The trivalent rare earth (RE^{3+}) doped UC luminescent materials are the topics of extensive investigations due to their attractive applications in display devices, cell imaging, lasers, temperature sensor and so on [1–5]. Recently, optical thermometry techniques based on RE^{3+} doped UC luminescent phosphors have drawn increasing attentions, since they can be used in some harsh environments, such as oil refineries, building fire detection and biocompatible temperature probe, etc [6–8]. Among them, FIR technique demonstrates the advantages of improved sensing sensitivity and reduced dependence on measuring conditions (i.e. fluorescence loss and pumping power fluctuation), which measures temperature via evaluating the temperature dependent FIR of two thermal coupled energy levels [7–9]. A lot of papers have reported that a larger energy gap between these thermal coupling levels gives rise to a higher temperature sensing sensitivity. However, since the energy gap between two thermal coupled levels is required to be 200–2000 cm^{-1}, further enhancement of the sensing sensitivity is restricted intrinsically [10]. To solve the drawback, several methods have been proposed by different researches, such as non rare earth ions doping, core-shell structure and so on [11–14]. But the usage of the FIR value from two non-thermal coupled levels of RE^{3+} ions for temperature sensing has received little attentions.

In this work, the temperature-dependent UC emissions from the solution combustion synthesized Tm^{3+}/Yb^{3+}: Y_2O_3 NPs under 980 nm excitation have been investigated. By employing the FIR technique, the temperature sensing behaviors are explored based on thermal coupled levels ($^1G_{4(a)}$ and $^1G_{4(b)}$) and non-thermal coupled levels ($^3F_{2,3}$ and $^1G_{4(b)}$) of Tm^{3+} ions, respectively. Meanwhile, the temperature-dependent emission color and luminescent thermal stability of the NPs are also the objectives for present research.

2. Experimental

Y_2O_3 NPs codoped with 0.5mol%Tm^{3+} and 5mol%Yb^{3+} ions were prepared by solution combustion method. The procedure is as follows: stoichiometric amounts of $Tm(NO_3)_3 \cdot 6H_2O$, $Y(NO_3)_3 \cdot 5H_2O$ and $Yb(NO_3)_3 \cdot 5H_2O$ were dissolved in de-ionized water. Glycine was added into the solution, and the mole ratio of nitrate to glycine

---

* Corresponding author.
** Corresponding author.
E-mail address: sxucjlu@163.com (S. Xu).

https://doi.org/10.1016/j.optmat.2018.01.039

is 1:3.5. The mixed solution was heated at 120 °C to get transparent gel. The gel was heated at 300 °C for 2 h and then calcined at 1200 °C for 2 h. XRD analysis was performed on a Bruker D2 PHASER Diffractometer with Cu-K$_\alpha$ radiation ($\lambda = 1.5406$ Å) in the 2θ range from 15° to 80°. TEM and high resolution TEM (HRTEM) observations were carried out using Tecnai G2 F20 at an operating voltage of 200 kV. The UC spectra were measured by a FLUOROLOG3/Jobin-Yvon spectrofluorometer under 980 nm continuous wave diode laser. The temperatures of the sample were adjusted by a temperature controlling system (TAP-02) and monitored by a copper-constantan thermocouple.

3. Results and discussion

XRD experiment reveals that all diffraction peaks are consistent with the JCPDS No. 65-3178 card for cubic Y_2O_3 phase (Fig. 1(a)). The average crystalline grain size of the NPs is calculated to be ~41 nm by Scherrer's equation. Fig. 1(b) and (c) illustrate that the sample exhibits a nearly spherical morphology with the average particle size of ~45 nm. The HRTEM image shows the (222) plane of cubic Y_2O_3 phase with interplanar spacing of ~3.06 Å (Fig. 1(d)). It further confirms that the particles are highly crystallized with no amorphous phase area.

The UC spectra of 0.5%Tm^{3+}/5%Yb^{3+}:Y_2O_3 NPs at different temperatures under a 980 nm diode laser excitation shown in Fig. 2(a) illustrate that the UC spectra include emission bands located at blue (477 and 490 nm) and red (655, 662 and 684 nm) regions. Fig. 2(b) shows the log-log plots of fluorescence intensity as a function of the excitation power. The fitted slope values are ~2.43 (477 nm), ~2.42 (490 nm), ~2.33 (655 + 662 nm) and ~1.72 (684 nm), respectively. It reveals that three photons are required for the population of $^1G_4$ level, while $^3F_{2,3}$ levels are populated by two photons processes.

The main UC photoluminescence mechanisms can be explained with the energy levels diagram (Fig. 2(c)). As Yb^{3+} ions have much larger absorption cross-section at 980 nm than Tm^{3+} ions, the energy transfer (ET) process from Yb^{3+} to Tm^{3+} ions is believed to be mainly responsible for the population of emitting levels of Tm^{3+} ions. As shown in Fig. 2(c), the Yb^{3+} ion in the ground-state can be excited to the $^2F_{5/2}$ level under 980 nm excitation. Then, the Tm^{3+} ion can be pumped from the ground state to the $^3F_{2,3}$ level via the sequential ET-1 and ET-2 processes. Some of the Tm^{3+} ions in the $^3F_{2,3}$ level can decay radiatively to the ground state and emit the photons around 684 nm. Meanwhile, other Tm^{3+} ions can relax nonradiatively to the $^3H_4$ level, which are further promoted to the $^1G_4$ level through the ET-3 process. Finally, the $^1G_4 \rightarrow {}^3H_6$ transition gives rise to the blue emissions (477 and 490 nm), while the $^1G_4 \rightarrow {}^3F_4$ transition leads to the fluorescence emissions around 655 and 662 nm. However, the slope values for the UC emission bands at 477 nm, 490 nm and 655 + 662 nm are observed to be lower than

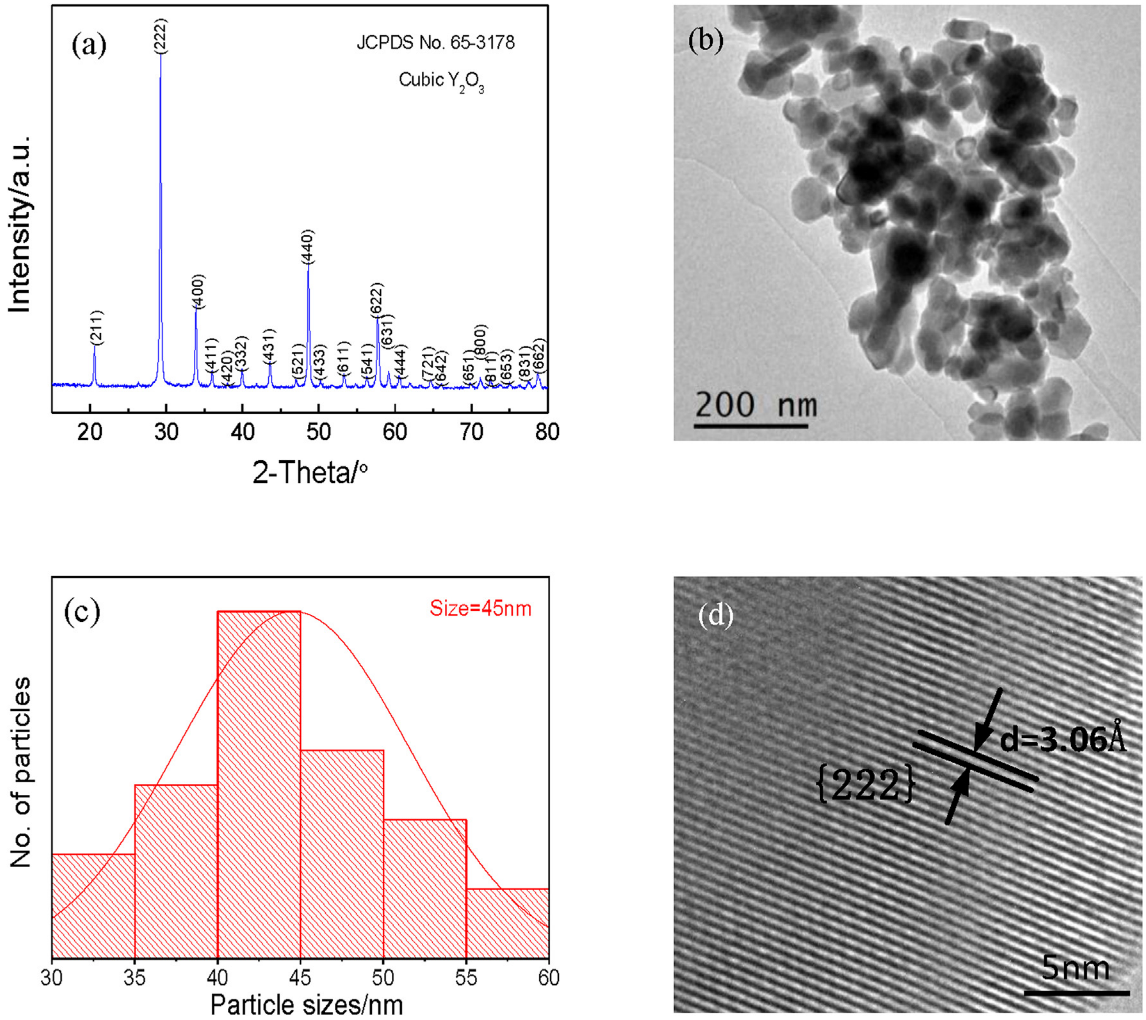

Fig. 1. XRD pattern (a), TEM image (b), size distribution histogram (c) and HRTEM image (d) of the prepared Tm^{3+}/Yb^{3+}:Y_2O_3 NPs.